International Journal of Science and Research (IJSR)
ISSN (Online): 2319-7064

Optical and Structural Properties of the Sm^{3+} Ions in Sodium Zirconium Silicate Glasses

V. Poli Reddy[1], M. Rami Reddy[2]

Department of Physics, Acharya Nagarjuna University, Nagarjuna Nagar-522 510, India

Abstract: ***the sm^{3+} ions doped sodium zirconium silicate glasses are synthesized by melt quenching technique. The glass samples are characterized by XRD, optical absorption, luminescence, FTIR and Raman spectral techniques. The XRD clearly suggested that the glass samples are fully amorphous in nature. The optical absorption and luminescence spectra are analyzed using Judd–Ofelt parameters for investigating ligand environment around sm^{3+} ions and these parameters are following the trend $\Omega_2>\Omega_4>\Omega_6$. The variation of band intensities attributes to the energy transfer through cross relaxation between sm^{3+} ions. From the radiate parameters, it is concluded that 0.4 mol% sm –doped glasses are efficient laser active materials. The different FT–IR and Raman spectra the assignments of the absorption bands are compiled which shows the gradual evolution of the rigid glassy network beyond Sm 4.***

Keywords: sodium zirconium silicate glasses, J–O parameters, polymerizations of network.

1. Introduction

Alkali silicate glasses have potentials applications as phosphors, IR fiber optics, laser windows, multifunctional non–linear optical devices, solar energy converters and in a number of electronic devices. Moreover they play an attractive role in the electrochemical applications such as power sources especially in the field of solid state batteries. On the other hand these glass systems also are used for testing generalized formulation of the modified Urbach's rule (MRU) [1-5].J. E. Shelby [6] investigated on difficulties on the synthesis of alkali silicate glasses, he concluded that the glasses containing less than ≈10 mol% alkali oxide are considerably more difficult to melt due to their high viscosities and metastable immiscibility occurred. In case of sodium silicate systems, immiscibility limits up to ≈ 20 mol%; to avoid the regions of metastable immiscibility, the Na_2O content in composition is taken up to 40 mol%. The mechanical properties the glasses are reinforced by the addition of zirconia (ZrO_2) to sodium silicate glasses; it improves the transparency, electrical resistivity and chemical inertness of glasses [7]. In view of all these fundamental aspects of sodium zirconium silicate glass offers good environment for hosting the luminescent rare earth (RE) ions also. The optical investigations of RE ions doped glasses are found to be extensive applications in the fields of lasers and telecommunications. In this direction a great amount of research has been carried out to develop new glass matrices containing rare–earth (RE) ions.

Among different rare earth ions, sm^{3+} ions containing glass networks exhibit a strong orange–red fluorescence in the visible region and they are of interest in lasers for next generation nuclear fusion. The spectral studies of sm^{3+} ion ($4f^5$) doped in glasses are complicated when compared with other rare earth ions [8-9]. Because the energy levels lying close to each other, it is difficult for the determination of meaningful intensity parameters needed in the calculation of various radiative properties. In the present work, we are investigating on the optimization of optical and structural properties of Sm^{3+} ion in sodium zirconium silicate glasses using XRD, Optical absorption, Luminescence, FT–IR, Raman spectral technique

2. Experimental Technique

The Table 1 illustrates the details of composition of the glasses used for present investigation. The glasses samples are synthesized by melt quenching technique. In this technique, appropriate amounts (all in mol %) of Na_2CO_3, ZrO_2, SiO_2 and Sm_2O_3 (analytical grade reagents) are powdered and thoroughly mixed in agate mortar. Then it is taken in the silica crucible after calcination and placed in an automatic temperature controlled furnace at a temperature range 1430–1450 ^{0}C for 20 min. The molten form of the material is poured on the brass mould for the required shape and then annealedat 475 ^{0}C for removing thermal stress in the glasses. Then the samples are finely polished to final dimensions 1cm×1cm×0.2 cm for the present measurements.

The X–ray diffraction spectrum is recorded on a diffractometer with copper target (XRDARLX'TRA) and nickel filter operated at 40 kV, 30 mA. The optical absorption (UV–Vis) spectra are recorded on JASCO, V–570 spectrophotometer from 200 to 1900 nm with spectral resolution of 0.1 nm. The luminescence spectra are recorded at room temperature from 500–750nm on a Photon Technology International (PTI) spectrofluorometer with excited wavelength 400 nm. Infrared transmission spectra are recorded on a JASCO–FT/IR–5300 spectrophotometer with resolution of 0.1 cm^{-1} in the spectral range 400–2000 cm^{-1} using KBrpellets (300 mg) containing pulverized sample (1.5 mg). The Raman spectra (model Nexus 670 Nicolet–Madison–W. I. USA)have been recorded on Fourier Transform Raman spectrometer with resolution of 4 cm^{-1}in the range 200–1400 cm^{-1}.

3. Results

The XRD spectra of glass are shown in the Fig 1. The spectra exhibits two broad bumps at about ~31^0 and ~40^0 (=2θ). No any other sharp peaks are observed which suggested random distribution of atoms in the glass matrix.

Figure 2: Illustrates the optical absorption spectra of specified glasses respectively. No absorption bands are

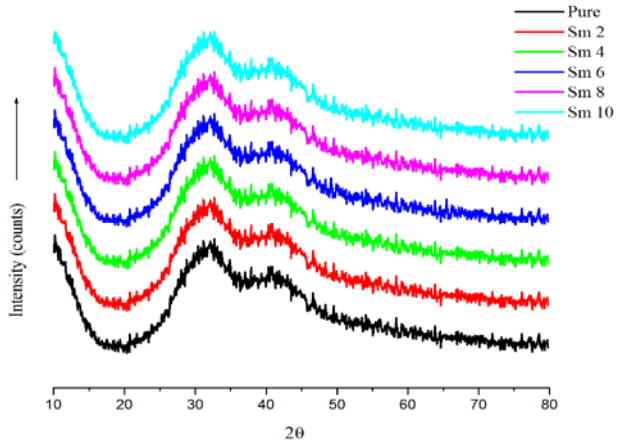

Figure 1: XRD spectra of glass

observed in the host glass. On the other hand Sm^{3+} ions are introduced into glass network; thirteen absorption bands are observed at about ~342, ~361, ~375, ~402, ~417, ~471, ~945, ~1069, ~1221, ~1354, ~1463, ~1521 and ~1585 nm [10-12]. These bands are originating from $^6H_{5/2}$ (ground state of sm^{3+}) and thebands assignments have been made on the basis of the Carnall et al [13-15]the transitions are given as follows

$^6H_{5/2} \rightarrow {}^4H_{9/2}$, $^4D_{3/2}$, $^6P_{7/2}$, $^6P_{3/2}$, $^6P_{5/2}+{}^4L_{13/2}$, $^4I_{13/2}$, $^6F_{11/2}$, $^6F_{9/2}$, $^6F_{7/2}$, $^6F_{5/2}$, $^6F_{3/2}$, $^6H_{15/2}$ and $^6F_{1/2}$ respectively

Interesting optical features are observed in the absorption spectra; here the intensity and half widths of all the bands are modified by the increasing contents of Sm^{3+} ions in the glass network. In glass network, the RE ions have all possible transition between the valence and conduction bands which are classified as direct, indirect transitions, these energy band gaps are evaluated by means of Tauc's plots is shown in the Fig 3 and 4as per the equation given below

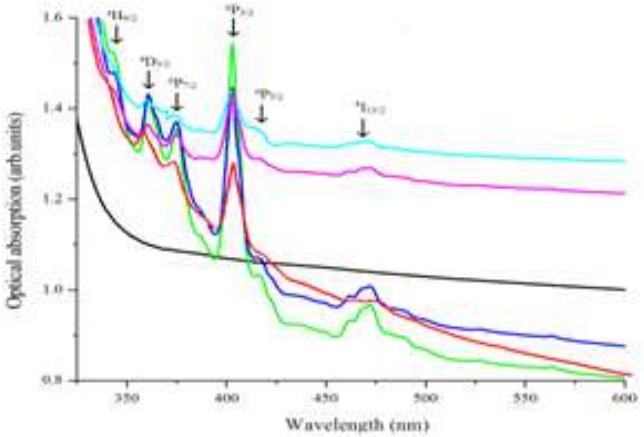

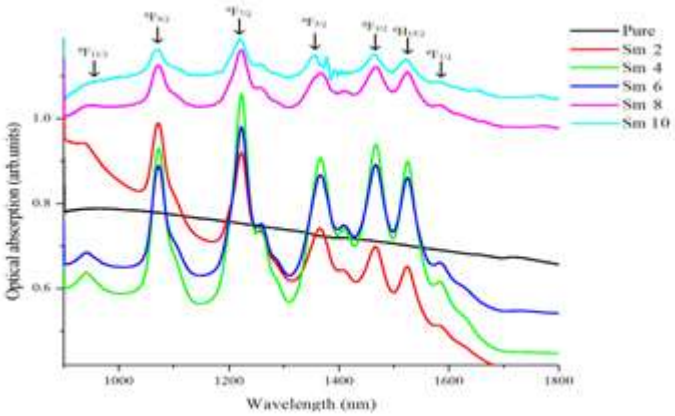

Figure 2: The otical absorption spectrum of specified glass

$$\alpha(\nu)h\nu = C\,(h\nu - E_o)^n$$

Here all terms have stranded meaning. The exponent (n) can take values 2 and 1/2 for indirect, direct transitions in glasses respectively. The cut off wavelength along with energy band gaps are mention in the Table 2. Herethe sample Sm4 hasminimum optical band gap energy when compared with remaining. The J–O Theory is successfully applied and the oscillatory strengths of the bands are presented in the Table 3.

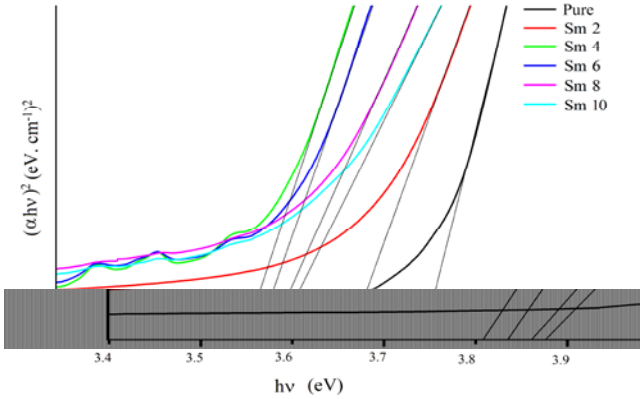

Figure 3: Tauc's plots for direct band gap

Fig 5 shows the luminescence spectra, here four prominent intensive emission bands are observed at about ~565, ~603, ~650 and ~709 nm and these bands are assigned to $^4G_{5/2} \rightarrow {}^6H_{5/2}$, $^4G_{5/2} \rightarrow {}^6H_{7/2}$, $^4G_{5/2} \rightarrow H_{9/2}$ and $^4G_{5/2} \rightarrow H_{11/2}$ transitions of sm^{3+} ions in the glass matrices [16-19]. Here the intensities of the emission bands are gradually increased up to 0.4 mol% of sm^{3+} ions further increasing an interesting converse trend is observed.

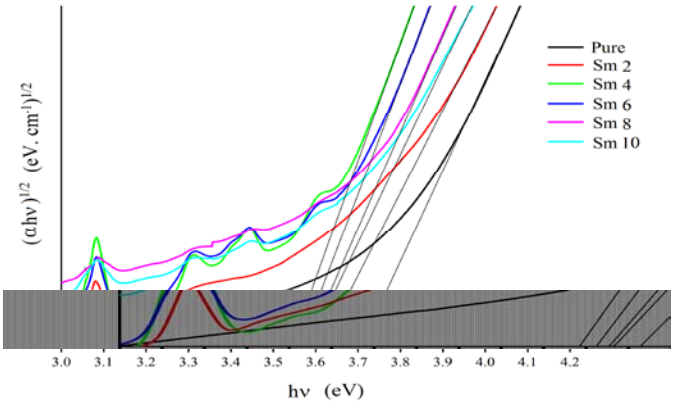

Figure 4: Tauc's plots for direct band gap

Table 5 represents radiative probability and branching ratios of the transitions.

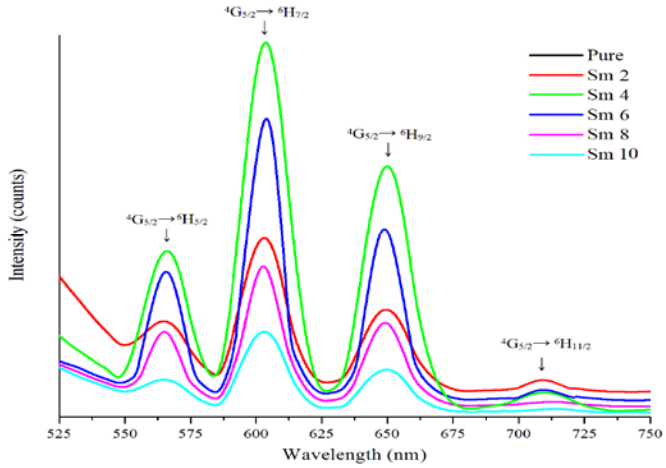

Figure 5: shows the luminescence spectra

Fig 6 and 7represents FTIR and Raman spectra of specified samples. In FTIR spectra we observed five bands at about ~467, ~743, ~800, ~962 and ~1086 cm^{-1}[20-23]. These bands are assigned to Characteristic vibrations of Zr-O/ deformed vibrations of Si-O, Zr-O-Zr vibrations/ ZrO_4 units, Symmetrical bending vibrations of $[SiO_4]^{4-}$ units, Rocking vibrations of Zr-O-Si, Asymmetric stretching vibrations of Si-O in the glass matrix. On the other hand in the Raman spectra we observe four Raman bands are observed and are given as ~354, ~645, ~948 and ~1090 cm^{-1}[21, 23]. All these bands are assigned to different structural units in the glass matrices and it is clearly given in Table 6. When the concentration of sm^{3+} ions in the glass network an interesting changes are observed and are given as follows

1. Structural units in the glass matrices and it is clearly given in Table 6. When the concentration of sm^{3+} ions in the glass network an interesting changes are observed and are given as follows
2. Both in FTIR and Raman, the asymmetric signal intensities (~1086 cm^{-1} /~1090 cm^{-1}) are gradually increased up to sm 4, beyond it reversal trend is observed. At the same time, the symmetrical vibrations at ~800 cm^{-1}/~645 cm^{-1}exhibits converse trend during Sm^{3+} ions doping in the glass matrix.
3. Rocking vibrations of Zr-O-Si are increasing with Sm^{3+} ions content in the glass.

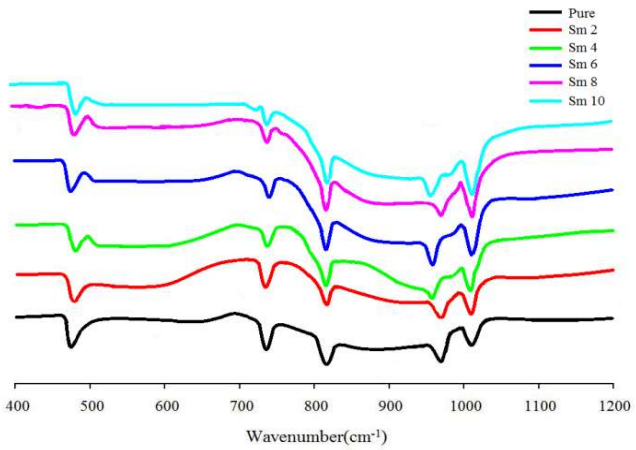

Figure 6: FTIR spectra of glass samples

4. Discussion

The $Na_2O–ZrO_2–SiO_2:Sm_2O_3$ glasses are an admixture of glass formers and modifiers. SiO_2 is one of the most common glass formers. Usually the Si atom shows tetrahedral coordination, with 4 oxygen atoms surrounding a central Si atom $[SiO4/2]^0$. The modifiers Na_2O, ZrO_2break the Si–O–Si linkage and cost to form Si–O termination. On the other hand Sm_2O_3 are also serves as a modifier because the radius of samarium ions is too large to enter the network. Thus, the structure is become depolymerized. These modification leads to the formation of metasilicates, pyrosilicates, and orthosilicates in the order: $[SiO_{4/2}]^0$, $[SiO_{3/2}O]^-$, $[SiO_{2/2}O_2]^{2-}$, $[SiO_{1/2}O_3]^{3-}$, and $[SiO_4]^{4-}$ which are designated as Q_4, Q_3, Q_2, Q_1, and Q_0, respectively [24-28].

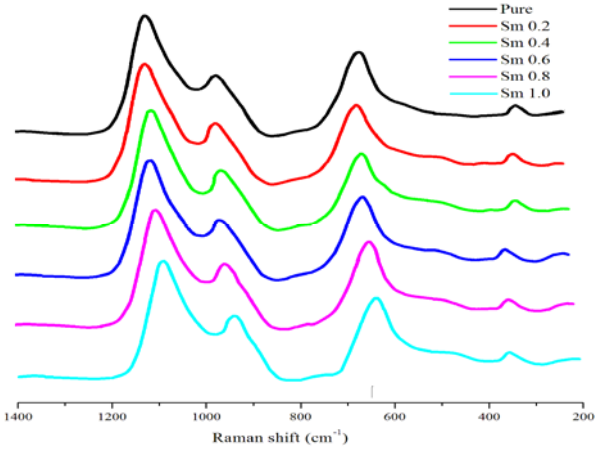

Figure 7: Raman spectra of glass samples

In the optical absorption spectra, Sm^{3+} ions in the glasses are responsible for the spectra due to the intraconfigurational transitions within incompletely filled 4f shell. Moreover the influence of the host lattice on the optical transitions within $4f^n$ configuration is small but essential. In the optical absorption spectra, the bands intensities are gradually increased with increasing concentration of sm^{3+} ions up to 0.4 mol %; further increasing, reversal trend is observed. This decrease is due to self–quenching of the via exchange of energy to the neighboring ground state sm^{3+} ions or host atoms in glasses with higher concentrations of the rare earth ions.

The spectral intensities for the observed bands in the optical absorption spectra are often expressed in terms of oscillator

strength (f). They can be expressed in terms of molar extinction coefficient (ε) and energy of the transition in wave number (υ) as

$$f_{exp}=4.32\times10^{-9}\int \varepsilon(\upsilon)\, d\upsilon \ldots\ldots\ldots..(1)$$

Judd and Ofelt independently derived expression for the oscillator strength of the induced electric dipole transition. It can be represented as a linear combination three Judd–Ofelt parameters (Ω_2, Ω_4 and Ω_6) and given as

$$f_{ed} = \frac{\upsilon}{(2j+1)}\left[\frac{8\pi^2 mc}{3h}\frac{(n^2+2)^2}{9n}\right]\sum_{\lambda=2,4,6}\Omega_\lambda < \psi_j\|U^\lambda\|\psi_j > \ldots\ldots\ldots\ldots (2)$$

$< \psi_j\|U^\lambda\|\psi_j >$are the reduced matrix elements of unit tensor operators and it is insensitive to the ion environment in the glass. Remaining all the terms in the above equations have standard meaning, we have used the values of the matrix elements as given by Carnallet al [13-15]Table 4 represents the J–O intensity parameters for all the glasses. Here the J–O parameters (Ω_λ) are calculated using least squares fitting manner and the estimated values are in the order of Ω_2=4.93x10^{-20} cm^{-2}, Ω_4=3.58x10^{-20} cm^{-2}, Ω_6=1.49x10^{-20} cm^{-2} (Sm2).Here Ω_2 is found to be higher and it is stand for the symmetry and the distortion associated to the structural change in the vicinity of Sm^{3+} ions. In the glass matrix, the average Sm–O distance is reduced due to stronger electrostatic attraction between cation (Si^{4+}, Zr^{4+} and Na^{+}) and anion (O^{2-}). As result the ligand field around Sm^{3+} ions becomes strong and causing higher value of Ω_2.

Luminescence spectra give detailed information about energy levels splitting of dopant ions in Na_2O–ZrO_2–SiO_2–Sm_2O_3 glasses. Luminescence spectra of Sm^{3+} are similar to those reported for a number of other glass systems. High intensive luminescence bands are observed in Sm4 glass. Further the decrease of band intensities at high concentration is due to self–quenching of the luminescence via exchange or ion pair relaxation mechanisms in glasses. The transfer of energy from the excited state of sm^{3+} ion by electric multipole interaction to neighboring sm^{3+} ion lying in the ground state is clearly shown in Fig 8.

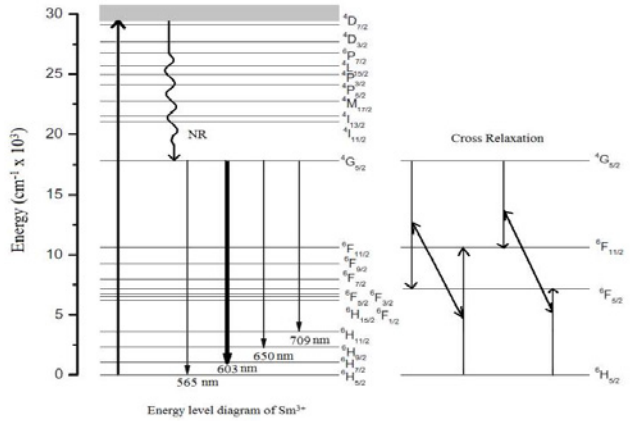

Figure 8: Energy level diagram of Sm^{3+} ion

Here the cross relaxation may takes palace ($^4G_{5/2} \rightarrow {}^6F_{5/2}$) to ($^6F_{11/2} \rightarrow {}^6H_{5/2}$) and ($^4G_{5/2} \rightarrow {}^6F_{11/2}$)to ($^6F_{5/2} \rightarrow {}^6H_{5/2}$) as the energy differences between these transitions are negligible. Luminescence efficiency is often represented in terms of branching ratio (β) and it is highest for $^4G_{5/2} \rightarrow {}^6H_{7/2}$ (~50%). Further Sm4 has highluminescence efficiency when comparison with other. The color space chromaticity diagram is shown in Fig 9and the color coordinates x and y values of all the investigated glass samples are mentioned in Table 7. The color chromatic diagram is also suggests Sm4 is best suited glass composition for orange-red emission.

FTIR and Raman spectra are non-destructive technique for investigating nature of the bonds in the glass matrix. The introduce of Sm_2O_3 by replacing Na_2O in the

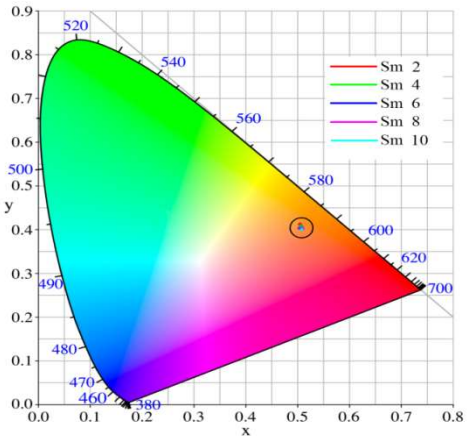

Figure 9: The color space chromaticity diagram

glass network, here asymmetric stretching vibrations of Si-O signal strength is gradually reduced up to Sm 4 then reversal tend is observed; this may be due to modifier action of Sm_2O_3, Na_2O in the glass matrix which disturb Si-O-Si, Zr-O-Zr network strongly to forms NBO by causing depolymerization and Sm^{3+} ions cannot enter into the matrix due to large radius. Then gradual increase of Sm_2O_3 beyond 0.4 mol%, Sm^{3+} ions interact with the local fields in the glass network. As a result, the electron distribution around Si^{4+}, Zr^{4+} get modification which leads to the formation of Si–O–Zr by replacing Si-O-Si, Zr-O-Zr. Therefore the network connectivity is gradually increased. These trends also supported by the optical band gaps of the specified samples. All the results reveals that the network become polymerized at higher concentration (beyond 0.4 mol%).

5. Conclusions

Optical and structural investigations of the Sm^{3+} ions doped sodium zirconium silicate glasses have been studied.XRD spectra reveal the glass network is fully amorphous in nature. Optical investigations, the Judd–Ofelt theory could successfully be applied to characterize the optical absorption spectra; out of the three J–O parameters, the value of Ω_2 is observed to be highest which suggests that highest covalent environment is present around Sm^{3+} ions. These glasses are suitable for strong orange – red emission. Structural properties reveals that the glass network becomes polymerizes beyond 0.4 mol% of sm^{3+} ions in the glass matrix.

Reference

[1] E.K.P.S. Lee, J. Ma, J. Euro. Ceram. Soc. 30 (2010) 1139.
[2] R. Baetens, B.P. Jelle, A. Gustavsen, Sol. Energy Mater. Sol. Cells 94 (2010) 87.

[3] H. A. Schaeer, Phys. Status Solidi A 22 (1974) 281.
[4] Fanderlik, Silica Glass and its Applications, Elsevier, Amsterdam, 1991.
[5] K.V. Arun, Fundamentals of Inorganic Glasses, Academic Press, NY, 1995. pp. 2, 4.
[6] E.M.M. Ewais, M.A.A. Attia, R.K. Bordia, Ceram. International 36 (2010) 1327.
[7] C. Siligardi, J.P. Wu, A.R. Boccaccini Materials Letters 60 (2006) 1607–1612
[8] K.K. Mahato, D.K. Rai, S.B. Rai, Solid State Commun. 108 (1998) 671.
[9] J.R. Schoonover, Y.L. Lee, S.N. Su, S.H. Lin, L. Eyring, Appl. Spectrosc. 28 (1984) 154.
[10] B.H. Rudramadevi, S. Bhuddhudu, Indian J. Pure Appl. Phys. 46 (2008) 825–832.
[11] H. Tanaka, T. Honma, J. Phys. Chem. Solids 64 (2003) 1179–1184.
[12] C.K. Jayasankar, P. Babu, J. Alloys Compd. 307 (2000) 82–95.
[13] W.T. Carnall, G.L. Goodman, J. Chem. Phys. 90 (1989) 3443–3457.
[14] W.T. Carnall, H. Cross white, Energy level Structure and Transition Probabilities of the Trivalent Lanthanides in LaF_3, Argonne National Laboratory Report, Argonne, Illinois, 1977.
[15] W.T. Carnall, P.R. Fields, J. Chem. Phys. 49 (1968) 4424–4442.
[16] M.B. Saisudha, j. Ramakrishna, Opt. Mater. 18 (2002) 403–417.
[17] T. Suhasini, L. RamaMoorthy, Opt. Mater. 31 (2009) 1167–1172.
[18] D.H. Dho, K. Hirao, J. Non-Cryst. Solids 215 (1997) 192–200.
[19] R. Krsmanovic, Z. Antic, J. Alloys Compd. 505 (2010) 224–228.
[20] M. Nakamura, Y. Mochizuki, K. Usami, T. Nozaki, Solid State Commun.50 (1984) 1079.
[21] Y. Yu, X. Wang, Y. Cao, X. Hu, Appl. Surf. Sci. 172 (2001) 260.
[22] T. Uma, M. Nogami, J. Membr. Sci. 334 (2009) 123.
[23] T. Srikumar, I.V. Kityk, N. Veeraiah, Ceram. Int. 37 (2011) 2763
[24] G. Srinivasarao, N. Veeraiah, J. Solid State Chem. 166 (2002) 104.
[25] F.H. ElBatal, Y.M. Hamdy, J. Non-Cryst. Solids 355 (2009) 2439.
[26] V. Sudarsan, V.K. Shrikhande, J. Phys.: Condens. Matter 14 (2002) 6553.
[27] W. Wang Paul, Lipeng Zhang, J. Non-Cryst. Solids 194 (1996) 129.
[28] E. Baiocchi, A. Montenero, M. Bettinelli, J. Non-Cryst. Solids 46 (1981) 203

Tables 1: Glass compositions

Glasses	*Na_2O*	*ZrO*	*SiO_2*	*Sm_2O_3*
	Mol %	*Mol %*	*Mol %*	*Mol %*
Pure	40.0	5.0	55.0	-
Sm 2	39.8	5.0	55.0	0.2
Sm 4	39.6	5.0	55.0	0.4
Sm 6	39.4	5.0	55.0	0.6
Sm 8	39.2	5.0	55.0	0.8
Sm 10	39.0	5.0	55.0	1.0

Table 2: Optical band gaps of the glasses

Glasses	*Cut off wavelength*	*Optical band gap (eV)*		
		Direct	*Indirect*	*Theoretical*
Pure	339	3.7498	3.7021	3.6010
Sm 2	341	3.6652	3.6275	3.6427
Sm 4	351	3.5567	3.5471	3.5389
Sm 6	350	3.5692	3.5670	3.5491
Sm 8	350	3.5759	3.5703	3.5491
Sm 10	349	3.5890	3.5810	3.5592

Table 3: Theoretical and experimental oscillatory strengths of Sm^{3+} doped sodium zirconium silicate glasses

Transition $^6H_{5/2}$ →	*Sm 2*		*Sm 4*		*Sm 6*		*Sm 8*		*Sm 10*	
	f_{cal} (x 10^{-6})	*f_{exp} (x 10^{-6})*	*f_{cal} (x 10^{-6})*	*f_{exp} (x 10^{-6})*	*f_{cal} (x 10^{-6})*	*f_{exp} (x 10^{-6})*	*f_{cal} (x 10^{-6})*	*f_{exp} (x 10^{-6})*	*f_{cal} (x 10^{-6})*	*f_{exp} (x 10^{-6})*
$^4D_{3/2}$	1.1	1.1	1.1	1.1	1.1	1.1	1.1	1.1	1.0	1.0
$^6P_{7/2}$	0.8	0.8	0.8	0.8	0.8	0.8	0.8	0.8	0.7	0.7
$^6P_{3/2}$	3.5	3.5	3.6	3.6	3.5	3.5	3.4	3.4	3.3	3.3
$^6P_{5/2}$	0.2	0.2	0.2	0.2	0.2	0.2	0.2	0.2	0.2	0.2
$^4I_{13/2}$	0.5	0.5	0.5	0.5	0.5	0.5	0.4	0.4	-	0.0
$^6F_{11/2}$	0.2	0.2	0.2	0.2	0.1	0.1	0.1	0.1	-	0.0
$^6F_{9/2}$	2.3	2.3	2.4	2.4	2.0	2.0	2.0	2.0	2.0	2.0
$^6F_{7/2}$	3.2	3.2	3.3	3.3	3.1	3.1	3.1	3.1	3.2	3.3
$^6F_{5/2}$	1.8	1.8	2.0	2.0	2.2	2.2	2.2	2.2	2.2	2.2
$^6F_{3/2}$	1.9	1.9	2.1	2.1	1.3	1.3	1.4	1.3	1.3	1.3
$^6H_{15/}$	1.6	1.6	1.6	1.6	0.4	0.4	0.4	0.4	0.4	0.4
$^6F_{1/2}$	0.3	0.3	0.4	0.4	0.6	0.6	0.6	0.6	-	0.6
Rms deviation	0.1173		0.0984		0.1118		0.1092		0.2821	

Table 4: J-O parameters of glasses

Glasses	*$\Omega_2 x10^{-}$*	*$\Omega_4 x10^{-}$*	*$\Omega_6 x10^{-20}$*
Sm 2	4.93	3.58	1.49
Sm 4	4.86	3.46	1.45
Sm 6	4.74	3.42	1.41
Sm 8	4.68	3.38	1.38
Sm 10	4.58	3.36	1.32

Table 5: Various radiative properties of Sm^{3+} doped sodium zirconium silicate glasses

Trans	*Sm 2*		*Sm 4*		*Sm 6*		*Sm 8*		*Sm 10*	
$^4G_{5/2}$	*A*(s	*β*	*A*(s	*β*	*A*(s	*β*	*A*(s	*β*	*A*(s	*β*
$^6H_{5/2}$	28.	6.	28.	6.	27.	6.	27.	6.	26.	6.
$^6H_{7/2}$	214	50	208	50	210	50	211	50	209	51
$^6H_{9/2}$	116	27	111	26	118	28	113	26	110	26
$^6H_{11/2}$	68.	16	65.	15	62.	14	69.	16	63.	15
$A_T(s^-$	428.41		414.54		419.94		421.51		409.99	
τ_R(ms	2.33		2.41		2.38		2.30		2.44	

Table 6: FTIR and Raman spectral data

FT IR bands (cm^{-1})	*Raman bands (cm^{-1})*	*Band assignment*
-	~354	Rocking vibrations of Si-O-Si
~467	-	Characteristic vibrations of Zr-O/ deformed
~743	-	Zr-O-Zr vibrations/ ZrO_4 units
~800	~645	Symmetrical bending vibrations of $[SiO_4]^{4-}$ units
~962	~948	Rocking vibrations of Zr-O-Si
~1086	~1090	Asymmetric stretching vibrations of Si-O

Table 7: Color intensity coordinates

Glass	*The chromaticity*	
	x	*y*
Sm 2	0.5088	0.3962
Sm 4	0.5184	0.3956
Sm 6	0.4946	0.3992
Sm 8	0.5044	0.3987
Sm 10	0.5037	0.3965

Author Profile

V. Poli Reddy received M. Sc (Physics) and M.Phil degrees from Acharya Nagarjuna University, Guntur, India, with first class in the years 2003 and 2007 respectively. He is a being has participated in number of seminars workshops and published nearly 02 papers. Presently he is pursuing Ph. d (Glass Science) from Acharya Nagarjuna University.

Dr. M. Rami Reddy is Assistant Professor in Acharya Nagarjuna University. His areas of specialization are Glass Science, Solid State Spectroscopy and Nano Materials. He has 23 International publications (Peer Reviewed). He has attended 20 conferences/ seminars/ workshops. Under her guidance three- Ph. D, eight -MPhil are awarded and five more Ph. D's and three more M. Phil are pursuing.